# Phase Separation and Morphology in Ethylcellulose/ Cellulose Acetate Phthalate Blends

**P. SAKELLARIOU**[*,1] **and R. C. ROWE**[2]

[1]ICI Paints, Wexham Road, Slough, United Kingdom, [2]ICI Pharmaceuticals, Alderley Park, Macclesfield, Cheshire, United Kingdom

## SYNOPSIS

This article discusses the phase separation and morphology of ethylcellulose/cellulose acetate phthalate blended films cast from methanol/methylene chloride (50/50 v/v) solvent mixture. The solvent system has been shown to be a cosolvent for CAP and a solvent/ nonsolvent for EC. The two polymers have been shown to phase separate for all blend compositions via nucleation and growth. The morphology of these systems consists of a dispersion of broad size distribution of the minor component in a matrix of the major one. The formation of two layers due to coalescence of the dispersed phases and their eventual precipitation has been observed for the middle blend compositions. Finally, the phase separation in this system is discussed in terms of the Flory–Huggins theory and changes in the solvency mechanism during film casting. Enrichment of the solvent system in methanol at relatively early stages of film casting leads to changes in the system viscosity, relative chain conformation in solution, and chain diffusion. The effect of these parameters on the final morphology are discussed in terms of deviations from the equilibrium binodal decomposition.

## INTRODUCTION

Controlled release through polymeric matrices has attracted considerable attention over recent years. The release profile is controlled by the chemical nature and morphology of the polymeric matrix and by the overall device shape. Significant advancements have been achieved in both the understanding of the physical chemistry of controlled release and in the synthesis of specialized polymer systems.[1,2] Despite the number of published data there has been no systematic study on the phase separation and morphology aspects of controlled release. Early studies on films concentrated on the relationship between the size of the pores available for drug diffusion and the drug release profile.[3,4] Little or no attention has been focused on the underlying interactions in the multicomponent polymer matrix and, more important, the control of its morphology. We will be attempting, in a series of publications, to

address this issue in blended cellulose ethers and esters films.

Blends of ethylcellulose with pH-dependent soluble polymers are widely used in the formulation of delayed or sustained release films.[5] Cellulose acetate phthalate is readily water-soluble at pH greater than 7, and is therefore used for drug targeting at the upper part of the small intestine.

In the absence of specific interactions, most polymer blends are incompatible. This is a direct result of the negligible entropy of mixing, which cannot compensate for the usually unfavorable contribution of the enthalpy of mixing to the free energy of mixing.[6] In earlier publications we reported data on the compatibility of ethylcellulose with a number of cellulose ethers, esters, and polyethylene glycol.[7] Morphologies were suggested for these systems based upon studies of changes in the polymeric interactions with the preferential dissolution of the water-soluble component from the blend.[8] We now report more detailed data on the compatibility and morphology of ethylcellulose/cellulose acetate phthalate blends. We also attempt to correlate changes in the

solvency mechanism during film casting to the morphologies of the films.

## EXPERIMENTAL

The water insoluble polymer studied was ethylcellulose (EC, Grade N50) supplied by Hercules Powder Inc. The pH-dependent-water-soluble polymer, cellulose acetate phthalate (CAP), was supplied by Eastman Chemical Products. Both polymers have the same backbone consisting of the anhydroglucose unit of cellulose with different substituent groups. Their structure can be depicted as follows:

$$\left[\begin{array}{c} CH_2OR \\ O \\ OR \\ OR \end{array}\right]_n$$

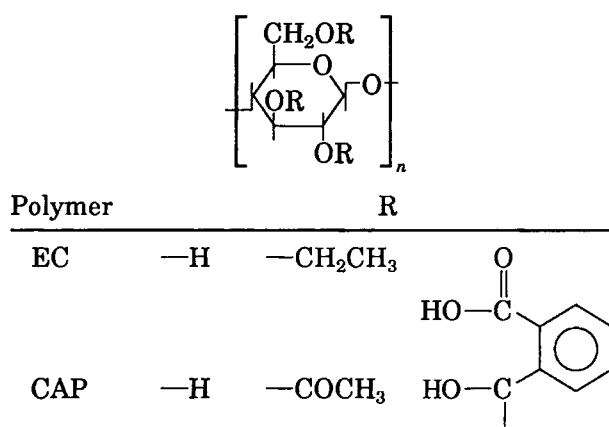| Polymer | | R | |
| --- | --- | --- | --- |
| EC | —H | —CH$_2$CH$_3$ | |
| CAP | —H | —COCH$_3$ | HO—C |

Table I illustrates the degree of substitution for the two polymers. Both were used as received. The molecular weight of EC ($\bar{M}_n = 53.3 \times 10^3$ g mol$^{-1}$) was determined by gel permeation chromatography (GPC) with dimethyl acetamide (DMA) as the carrier solvent. The GPC column was calibrated with polystyrene standards. CAP presented considerable difficulties in the GPC analysis. DMA was used initially as the carrier solvent but the chromatograph showed two completely separated molecular weight fractions; one of them was eluted at very short times. We believe this occurred because of limited solubility of CAP in DMA. When the carrier solvent was changed to tetrahydrofuran (THF), the polymer passed through the column almost immediately,

**Table I    Degree of Substitution for EC and CAP (% w/w)**

| Polymer | Ethoxy | Phthalyl | Acetyl |
| --- | --- | --- | --- |
| EC | 48–49.5 | — | — |
| CAP | — | 30–36 | 10–23.5 |

which showed poor solubility. We have therefore used an estimated molecular weight ($\bar{M}_n \cong 60 \times 10^3$ g·mol$^{-1}$) based upon cellulose derivatives with comparable film forming properties. The solvent used was a 50/50 v/v mixture of dichloromethane and methanol, which has been shown to be the best solvent for the blend. The solvents were standard LR grade and they were used without any further purification.

### Techniques

Torsional braid analysis (TBA) was used to obtain the dynamic mechanical spectra of the blends. The instrument and inert support have been described in detail in an earlier publication.[9] The instrument monitors the response of a polymer-impregnated loose-glass-fiber braid to a sinusoidal strain with varying temperature at relatively constant frequency (ca. 1 Hz). The specimen was prepared by impregnating heat-cleaned (500°C) glass braids in the polymer solution (5%–10% w/v). The samples were dried in an air oven at 85°C to constant weight. The cellulose acetate phthalate was subsequently leached from the braids by immersing them into pH 7 buffer solution for ca. 15 h. The samples were dried at 85°C in an air oven. The weight loss during leaching was monitored gravimetrically. The weight loss data were reproducible to within 2%.

The phase diagrams were determined by allowing solvent system/polymer 1/polymer 2 mixtures to separate into two layers in carefully sealed tubes immersed in a water bath, thermostatted at 28 ± 1°C. The systems were left to reach equilibrium for two months. The position of the interface was monitored by means of a cathetometer. Equilibrium was judged to have been reached when the position of the interface did not change for two consecutive weeks. The composition of the two phases was determined by gravimetric analysis of accurately measured volumes. The procedure involved leaching away all the CAP by immersing the accurately weighed films of the top phase in pH 8.00 buffer solution for one week. Additional points in the phase diagram were obtained by titrating cloudy EC/CAP/solvent systems with 50/50 v/v methanol/methylene chloride in sealed tubes.

The morphology was studied with SEM and phase contrast microscopy. The films were cast from 7% w/v polymer solutions in glass petri dishes. The petri dishes were covered to slow down solvent evaporation and to allow near-equilibrium morphologies to be obtained. The remaining solvent was removed under vacuum at 80°C overnight. For the SEM

studies, the films were embedded in epoxy resin, trimmed to obtain a flat surface, and immersed in pH 8.00 buffer solution to leach out the CAP-rich phases. The leached surfaces were observed under the SEM. This technique proved successful only for samples with EC as the matrix. The structures of samples with CAP as the major phase collapsed under the SEM high vacuum conditions. Phase contrast microscopy used 10–15 μm thick samples cut normal and parallel to the bulk film surface. Microtoming was significantly hindered since we could not use a water trough to collect the microtomed sections. Despite the relatively increased thickness of some samples, the basic features of the morphology can be resolved in the optical micrographs.

Finally, the IR spectra of the cosolvent system and polymer/cosolvent mixtures were observed by means of a Bruker-IFS 48 FTIR spectrometer. The polymer concentration in all polymer solutions was 0.5% w/v. The solutions were tested using a KBr adjustable cell at a fixed optical pathlength (9.6 $\times$ 10$^{-4}$ cm).

## RESULTS AND DISCUSSION

### Dynamic Mechanical Spectroscopy

Both polymers were amorphous. Two $\alpha$ relaxations were recorded over the entire blend composition
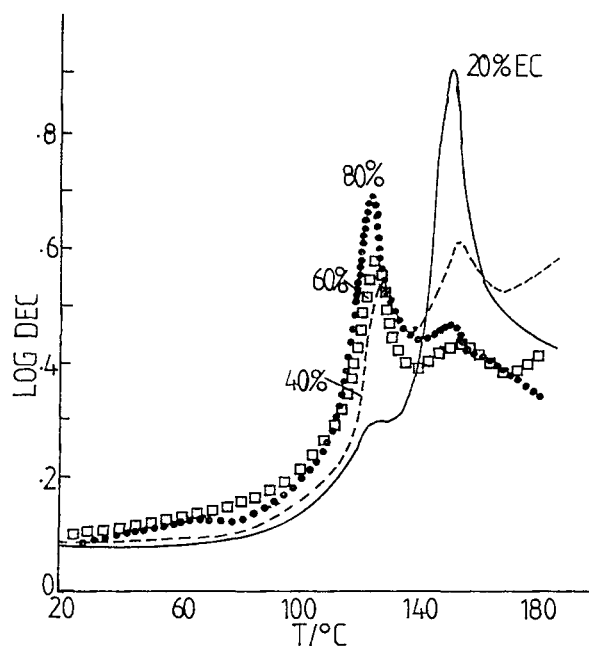


**Figure 1**  Dynamic mechanical spectra for EC/CAP blends.

range at temperatures close to the $T_g$ of EC and CAP (Fig. 1). The logarithmic decrement of the lower temperature relaxation decreased with the weight fraction of EC in the blend. The reverse trend was observed for the other relaxation. We, therefore, assign the relaxation at about 130°C to the EC-rich phase and the relaxation at about 150°C to the CAP-rich phase. The composition of the CAP-rich phase can be estimated by means of a simple equation derived by Fox,[10] assuming linear additivity of the free volumes of the two components. The Fox equation suggests the presence of 21% to 30% w/w EC in the CAP-rich phase (Table II). On the other hand, the $T_g$ of the EC-rich phase remains slightly below or at the $T_g$ of the EC homopolymer for all blend compositions. This shift in the $T_g$ is greater for samples with 20% and 40% w/w CAP (3.5–4°C) than for those with 60% and 80% w/w CAP (1.5°C). The shift for the latter systems becomes comparable to the accuracy of the TBA ($\pm1$°C), but is, nevertheless, reproducible. Our work on mixtures of EC with phthalyl plasticizers has already shown the presence of significant interactions between the $\sigma$-carboxy-benzoyl groups and EC.[11] We therefore suggest that the shift in the $T_g$ of the EC-rich phase is caused, at least in part, by the presence of some CAP in this phase. The phthalyl groups of the CAP introduce free volume lowering the $T_g$ of this phase and cancel out any contribution to the apparent $T_g$ from the $T_g$ of the CAP. It is interesting to note that increased mixing occurred at the two extreme blend compositions.

The dynamic mechanical spectra and weight loss data of the leached samples are shown in Figure 2. The two relatively sharp relaxations of the original spectra were replaced by a single relaxation close to the $T_g$ of the EC, and broadened toward higher temperatures. Only the system 20/80 w/w EC/CAP showed two distinct relaxations. On the other hand, the weight loss data suggest CAP retention throughout the blend composition. In view of these data we suggest that interactions between EC and the $\sigma$ carboxybenzoyl group of CAP are responsible for retention of some CAP. This is in agreement with the reported interactions between EC and a series of phthalate plasticizers[11] via the $\sigma$ carboxybenzoyl group.

### Phase Diagram

The experimentally determined phase coexistence curve (Fig. 3) is skewed toward EC, which suggests slightly lower solubility of this component in the solvent system. The system remains homogeneous

**Table II Dynamic Mechanical Data for EC/CAP Blends. $T_{g1}$ and $T_{g2}$ Correspond to the EC-Rich and CAP-Rich Phase Respectively**

| % w/w EC | $T_{g1}/°C$ | $T_{g2}/°C$ | $\Delta_{max}^1$ | $\Delta_{max}^2$ | % w/w EC/CAP |
|---|---|---|---|---|---|
| 100 | 131.5 | — | — | — | — |
| 80 | 127.0 | 153.5 | 0.70 | 0.47 | 28 |
| 60 | 128.0 | 156.0 | 0.59 | 0.44 | 21 |
| 40 | 130.0 | 155.0 | 0.54 | 0.61 | 24 |
| 20 | 130.0 | 153.0 | 0.30 | 0.91 | 30 |
| 0 | — | 163.0 | — | — | — |

throughout the blend composition at total polymer contents below ca. 9% w/v.

### Polymer Compatibility

The enthalpic contribution to the polymer–polymer interaction parameter can be calculated from a van Laar-type expression[12]:

$$\chi_{12} = (\delta_1 - \delta_2)^2 V_r/RT \qquad (1)$$

where $V_r$ is the reference volume ($cm^3 \ mol^{-1}$) and $\delta$ ($cal^{1/2} \cdot cm^{-3/2}$) is the solubility parameter. Krause's suggestion for the approximation of $V_r$ was adopted for the calculations.[13] The solubility parameters of EC and CAP can be calculated easily by means of the molar attraction constants (Table III).[13,14] The value for $\chi_{12}$ is thus calculated to be 1.03–1.72, depending upon the molar attraction constants used for the calculation of the solubility parameters (see Table III).[14] The critical interaction
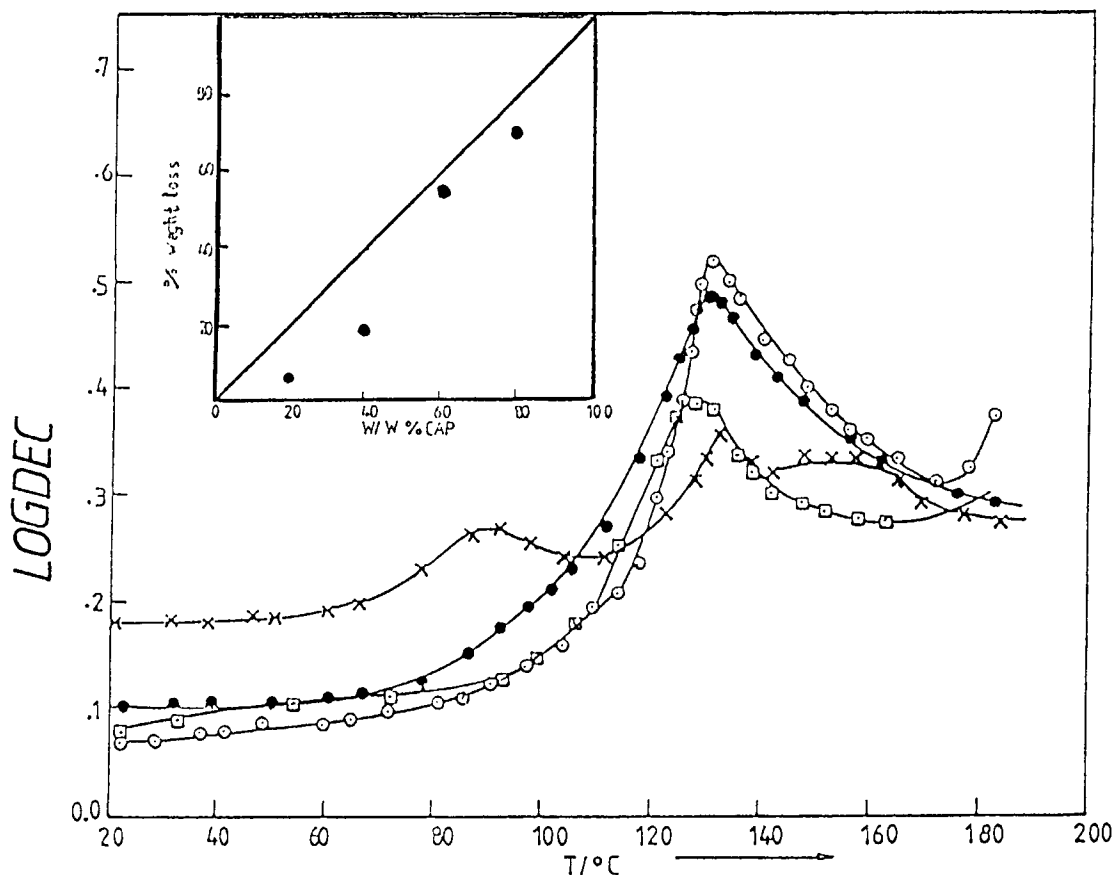


**Figure 2** Dynamic mechanical spectra and weight loss data for EC/CAP blends leached in pH 7 buffer for 15 hr.
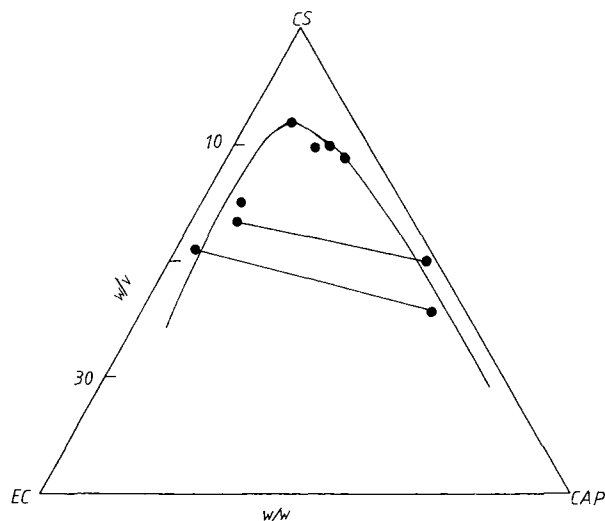
**Figure 3** Phase diagram of EC/CAP/(methylene chloride/methanol 50/50 v/v) system. CS denotes the solvent system.

parameter value for this system can be calculated from Flory's theory:

$$(\chi_{12})_{crit} = \tfrac{1}{2}(x_1^{-1/2} + x_2^{-1/2})^2 \qquad (2)$$

The polymer–polymer interaction parameter of the system is two orders of magnitude greater than the critical value (0.010), indicating a strong incompatibility drive in the system.[13]

This prediction is based upon the calculated solubility parameter data. Although it has been suggested that the data provide a good guide for polymer–polymer compatibility,[13] it would be interesting to use experimentally determined values for the polymer–polymer interaction parameter. The polymer–polymer interaction parameter can be calculated from the phase equilibria equations.[15] The Flory–Huggins equation for the free energy of a ternary system of two polymers and a single solvent reads:

$$\Delta G_m/RT = (n_1 ln\Phi_1 + n_2 ln\Phi_2 + n_3 ln\Phi_3)$$
$$+ (\chi_{12}\Phi_1\Phi_2 + \chi_{13}\Phi_1\Phi_3 + \chi_{23}\Phi_2\Phi_3)$$
$$(m_1n_1 + m_2n_2 + m_3n_3) \qquad (3)$$

The standard notation has been used. Subscripts 1, 2, and 3 denote the solvent system, EC, and CAP, respectively. The chemical potential of each blend component can be calculated in the traditional way[15] by differentiating equation (3) with respect to the

volume fraction of the corresponding component. The compositions of each conjugate phase can then be calculated by equating the chemical potential of each component in the conjugate phases. Narashimhan et al.[16] suggested the use of two adjacent tie lines of the experimental phase diagram to compute the polymer–polymer interaction parameter. Their treatment assumes that only the polymer–polymer interaction parameters change significantly with concentration within a narrow concentration range. The chemical potential equations for the two phases and the two tie lines ($I$, $II$) give, after rearrangement[17]:

$$\chi_{23}^{I}[(\Phi_2' - \Phi_2'') - (\Phi_1'' - \Phi_1')]^{I}$$
$$- \chi_{13}[(\Phi_2' - \Phi_2'') - (\Phi_1'' - \Phi_1')]^{I}$$
$$+ \chi_{12}[(\Phi_2' - \Phi_2'') + (\Phi_1'' - \Phi_1')]^{I}$$
$$= ln(\Phi_1''/\Phi_1')^{I} - (1/m_2)ln(\Phi_2''/\Phi_2')^{I} \qquad (4A)$$

$$\chi_{23}^{II}[(\Phi_2' - \Phi_2'') - (\Phi_1'' - \Phi_1')]^{II}$$
$$- \chi_{13}[(\Phi_2' - \Phi_2'') - (\Phi_1'' - \Phi_1')]^{II}$$
$$+ \chi_{12}[(\Phi_2' - \Phi_2'') + (\Phi_1'' - \Phi_1')]^{II}$$
$$= ln(\Phi_1''/\Phi_1')^{II} - (1/m_2)ln(\Phi_2''/\Phi_2')^{II} \qquad (4B)$$

$$\chi_{23}^{I}[(\Phi_3'' - \Phi_3') + (\Phi_1'' - \Phi_1')]^{I}$$
$$+ \chi_{13}[(\Phi_3'' - \Phi_3') - (\Phi_1'' - \Phi_1')]^{I}$$
$$- \chi_{12}[(\Phi_3'' - \Phi_3') + (\Phi_1'' - \Phi_1')]^{I}$$
$$= (1/m_3)ln(\Phi_3''/\Phi_3')^{I} - ln(\Phi_1''/\Phi_1')^{I} \qquad (4C)$$

$$\chi_{23}^{II}[(\Phi_3'' - \Phi_3') + (\Phi_1'' - \Phi_1')]^{II}$$
$$+ \chi_{13}[(\Phi_3'' - \Phi_3') - (\Phi_1'' - \Phi_1')]^{II}$$
$$- \chi_{12}[(\Phi_3'' - \Phi_3') + (\Phi_1'' - \Phi_1')]^{II}$$
$$= (1/m_3)ln(\Phi_3''/\Phi_3')^{II} - ln(\Phi_1''/\Phi_1')^{II} \qquad (4D)$$

**Table III Literature and Calculated Solubility Parameters for Methanol, Methylene Chloride, EC, and CAP (MPa$^{1/2}$)**

| Component | $\delta_p$ | $\delta_d$ | $\delta_h$ | $\delta$ | |
|---|---|---|---|---|---|
| Methanol | 12.3 | 15.1 | 22.3 | 29.7 | |
| Methylene chloride | 6.3 | 18.2 | 6.1 | 20.3 | |
| EC | — | — | — | 19.0[a] | 20.6[b] |
| CAP | — | — | — | 24.1[a] | 27.2[b] |

[a] Calculated from Hoy's molar attraction constants.[14]
[b] Calculated from van Krevelen's molar attraction constants.[14]

This is a system of four equations with four unknowns ($X_{12}, X_{13}, X_{23,II}$ and $X_{23,I}$), which can be solved numerically using a Gaussian elimination procedure. We must point out that the present theoretical treatment applies to ternary systems, while our system involves a mixed solvent system. We have treated the solvent system in our calculations as a single component of constant composition with polymer concentration and a single interaction parameter. Obviously this is a crude approximation; hence the qualitative rather than quantitative nature of the analysis. The values of polymer–polymer interaction parameters calculated with this procedure were 0.034 and 0.021 for systems at *ca.* 18% and 20% w/v total polymer concentration. The values, although numerically different from those predicted from the solubility parameters of the two polymers, are positive, indicating incompatibility of the two components. The polymer–polymer interaction parameter $((X_{23})_{pl})$ at the plait point of the phase diagram can be calculated from the equation derived by Scott[18]:

$$(X_{23})_{pl} = 1/2[m_2^{-1/2} + m_3^{-1/2}]^2(1 - \Phi_s)^{-1} \quad (5)$$

$(X_{23})_{pl}$ is calculated to be 0.038. The interaction parameters increase with increasing solvent volume fraction in agreement with earlier reports in the literature.[19,20,21]

## Morphology of EC/CAP Blends

Films cast under near equilibrium conditions were all cloudy, which confirmed phase separation for all blend compositions. The middle composition blends produced films which were separated into two layers. The top layer consisted of EC-rich matrix with CAP-rich dispersions. The morphology of the bottom layer was the mirror-image of the top one. The presence of the two phases is in agreement with the incompatibility observed in the TBA spectra. The composition of the two layers complies with the difference in the density of the two polymers ($d_{EC} = 1.13$ g cm$^{-3}$ and $d_{CAP} = 1.30$ g cm$^{-3}$). A broad distribution of the size of the dispersions was observed for all blend compositions (Figs. 4 and 5). This suggests that phase separation occurs through nucleation and growth. The maximum size of the dispersions was distinctly larger for systems with 40% and 60% w/w EC. The interfaces of the dispersions were sharp. The interface between the two bulk layers in the systems with 40% and 60% EC was sharp and the two layers separated readily during film handling. A number of samples were annealed above the $T_g$ of
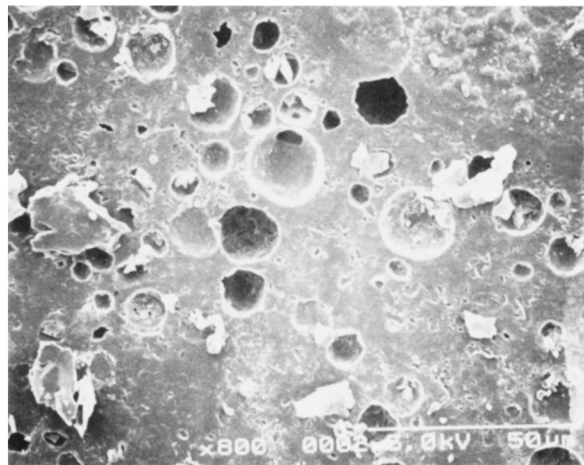
*A*
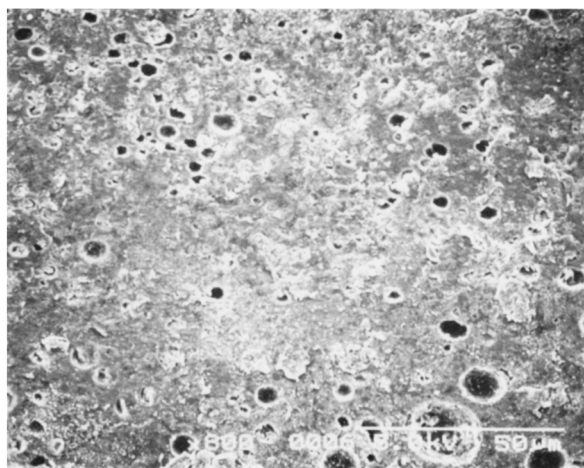
*B*

**Figure 4** Scanning electron micrographs of water etched surfaces for EC/CAP blends: (A) 60/40 w/w EC/CAP, Top layer, (B) 80/20 EC/CAP w/w.

both homopolymers (190°C) for 20–30 min. No significant change in film morphology was observed.

## SOLVENT PREFERENTIAL ADSORPTION AND SOLVENCY MECHANISM

The solvent system used in our studies introduces a further complication to the phase separation. EC dissolves in chlorinated hydrocarbons and some grades have been reported to swell slightly in alcohols. Alcohols have been shown to reduce the vis-
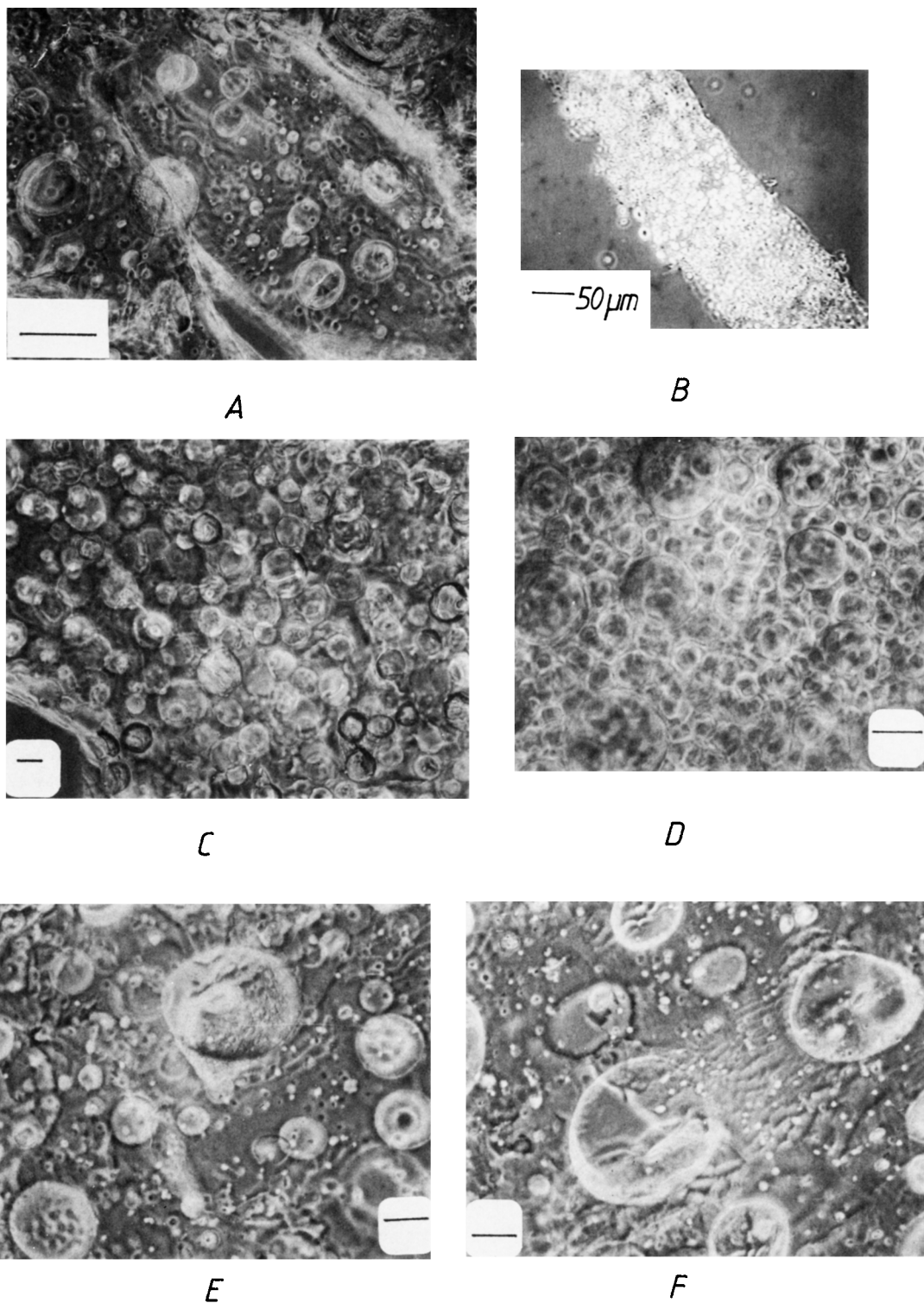
Figure 5 (a) Optical micrographs of cross-sections for EC/CAP blends: (A) 20/80 w/w EC/CAP; (B) 80/20 w/w; (C) 60/40 w/w EC/CAP Bottom layer; (D) 60/40 w/w Top layer; (E) 40/60 w/w Bottom layer; (F) 40/60 w/w Top layer. Bar = 25 μm.

cosity of EC solutions in chlorinated hydrocarbons. On the other hand CAP is insoluble in both chlorinated hydrocarbons and alcohols. It would, therefore, be expected that methylene chloride and methanol would show different adsorption characteristics with the two chains and, furthermore, that the

mechanism of solvation would be different for the two polymers.

The preferential adsorption can be studied by means of FTIR spectroscopy.[22] For a given solvent, the characteristic absorbance will vary with the extent of adsorbance/desorbance of the solvent on the polymer. The absorbance of the pure solvent will be:

$$A_0 = \alpha b c_0 \tag{6}$$

where $\alpha$ is the absorptivity, $b$ is the optical path length, and $c_0$ is the concentration. Addition of polymer to the solvent will change the absorbance to

$$A = \alpha b c \tag{7}$$

at the new solvent concentration; concentration $(c_0 - c)$ will give the amount of solvent adsorbed on the polymer chain. Consequently, negative sign of the difference $(A - A_0)$ will denote adsorption of the solvent on the polymer. Furthermore, the adsorption coefficient can be determined from:

$$b_1 = [x_1/M_3] m_3 \tag{8}$$

where $x_1 = (c_0 - c)/c_0$, $M_3$ and $m_3$ are the molecular weight of the polymer and the molecular weight of the repeat unit, respectively.

In our experiments, we kept both the optical path length $(9.6 \times 10^{-4}$ cm) and polymer concentration $(0.504\%$ g cm$^{-3})$ constant. The extinction coefficients for methanol and methylene chloride at the wavelengths of interest were determined using an adjustable liquid cell equipped with KBr windows. The accurate optical length was determined by the fringe method. The absorbances at 1268 cm$^{-1}$ and at 1029 cm$^{-1}$ were chosen to study the preferential adsorption in our systems. The former corresponds to $CH_2$—Cl and the latter to primary alcohol $CH_2$—OH. They were chosen because there was no significant overlap from one absorbance to the other. The characteristic absorbances for the polymer were not recorded because of the very low polymer concentration.

Table IV summarizes the changes in the IR absorption for 50/50 v/v methylene chloride/methanol mixtures with and without EC and CAP. The data suggest that the two polymers show different behavior for the two components of the solvent system. Methanol adsorbs on CAP but desorbs from EC. On the other hand, methylene chloride adsorbs on both polymers but also shows a much stronger adsorption on CAP. This is partly explained by the

**Table IV    Changes in the IR Absorption of Characteristic Bands for Methylene Chloride and Methanol in the Presence of EC and CAP**

| Sample | $(A_0 - A)$ | | $x^a$ | |
|---|---|---|---|---|
| | 1029 cm$^{-1}$ | 1268 cm$^{-1}$ | 1029 cm$^{-1}$ | 1268 cm$^{-1}$ |
| CAP | 0.0780 | 0.0183 | 4.94 | 3.84 |
| EC | −0.0881 | 0.0066 | −5.58 | 1.38 |

$^a$ $x$ denotes the $g$ adsorbed solvent per $g$ polymer.

presence of the pendant hydroxyl groups in CAP. We believe that these data have significant implications on the solvency mechanism in our system as well as the compatibility and morphology during solvent evaporation.

The system behavior is further complicated by changes in the solvent system composition during film casting. Figure 6 outlines these changes, ignoring any intermolecular interactions between methanol, methylene chloride, and the polymer molecules. The data represent solvent evaporation rates monitored gravimetrically in a closed container. Although it is not possible to relate the time scale of this experiment to that of the film casting procedure, it is apparent that the solvent system will be considerably enriched in methanol at relatively dilute stages of the process.

It is important to consider the differences in the solvation mechanisms for the two polymers for our solvent system in view of the FTIR data. The solvent system shows all the typical characteristics of cosolvency with respect to CAP. Although each component individually does not dissolve the polymer, their blend acts as a solvent. A simplistic explanation of the cosolvency can be based on the solubility parameter approach. The solubility parameter of the mixed solvent system can be calculated from reference 23:

$$\delta_{12} = [\delta_1 \Phi_1 + \delta_2 \Phi_2]/[\Phi_1 + \Phi_2] \tag{9}$$

The solubility parameter of methylene chloride/methanol mixture $(50/50$ v/v) is thus calculated to be 25 MPa$^{1/2}$, which is close to the predicted value for CAP $(\delta = 24.1$ MPa$^{1/2})$. Although this approach explains the behavior of the present system, it has been reported to fail in a number of other systems where cosolvency has been observed in cases with $\delta_1 > \delta_2 > \delta_3$ and $\delta_1 < \delta_2 < \delta_3$.[17] We believe that the approach proposed by Cowie and coworkers[24-28] offers a more comprehensive explanation. According to this approach the mechanism of cosolvency is
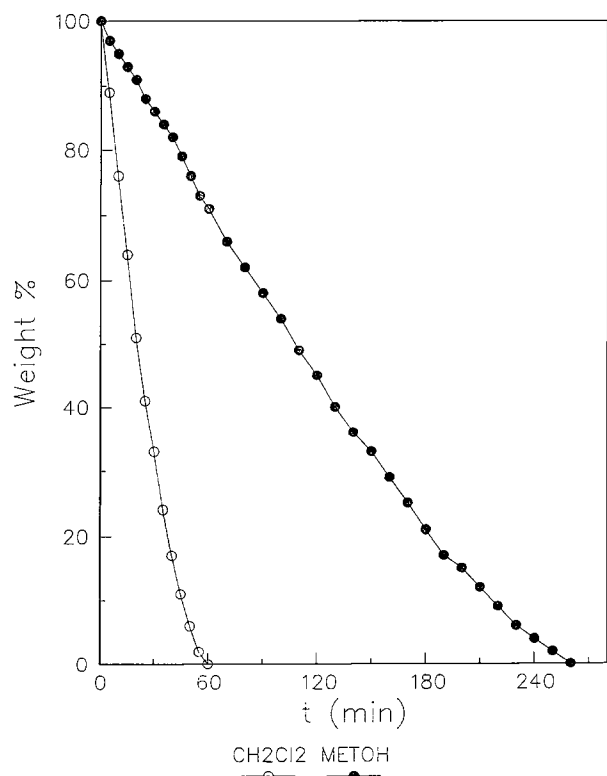
**Figure 6** Methanol and methylene chloride evaporation rates determined gravimetrically.

is enriched in methanol (1), the number of 1-2 contacts is reduced and the number fraction of 1-3 contacts is increased. A composition is soon reached when the number fraction of 1-3 contacts exceeds a critical value the polymer can tolerate and the polymer phase separates out of the solution.

EC, on the other hand, is preferentially solvated by methylene chloride, as shown by the FTIR data. This is also in agreement with the calculated solubility parameters (Table III). The solubility parameter of EC is much closer to that of methylene chloride than that of methanol. Methanol appears to alter the conformation of the chains in solution leading to reduced solution viscosity. The fact that the FTIR data show slight desorption of methanol from the polymer chain suggests that this is implemented mainly via modification of the polymer–methylene chloride interactions.

## Solvency and Phase Separation during Film Casting

Phase separation during film formation proceeds along the binodal curve. As the viscosity of the mixture increases, the time scale for diffusion of the molecules necessary for phase rearrangement be-
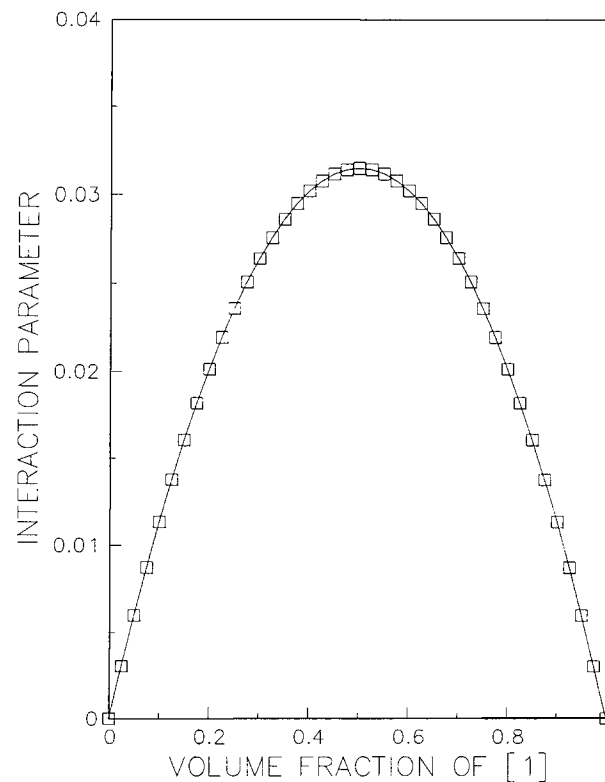
based upon the formation of energetically, relatively more favorable 1-2-3 contacts, which keep the polymer in solution. In this case the solvent–solvent interaction parameter becomes very critical because it regulates the extent of 1-2 contacts necessary to render contacts 1-2-3 energetically more favorable. Unfortunately $\chi_{12}$ for our solvent pair is not known. However, it can be calculated from

$$\chi_{12} = (V_{12}/RT)A_{12}\Phi_1\Phi_2 \qquad (10)$$

where $A_{12}$ is given from

$$A_{12} = (\delta_{p1} - \delta_{p2})^2 + (\delta_{d1} - \delta_{d2})^2$$
$$+ (\delta_{h1} - \delta_{h2})^2 \quad (11)$$

Figure 7 summarizes the effect of methanol volume fraction on the solvent–solvent interaction parameter. These data are in agreement with the experimentally determined molar excess Gibbs energy[29] and excess volume[30] variation with cosolvent composition. Both the calculated and the experimental set of data suggest that mixtures of ca. 50/50 v/v methylene chloride/methanol should be the best cosolvent system. As the cosolvent system



**Figure 7** Variation of the methanol–methylene chloride binary interaction parameter with composition.

comes comparable to, or even slower than, the time scale for concentration changes during film casting. This leads to deviations from the equilibrium binodal decomposition.[31,32] This process is further complicated in our case by the continuous change in the composition of the solvent system and, therefore, solvency of the two polymers. The solvent system is considerably enriched in methanol at relatively early stages of film casting. This is expected to have a significant effect on system viscosity, relative chain conformation, and, consequently, chain diffusion necessary for phase rearrangement. On the basis of our observation, EC chains will be expected to collapse at relatively earlier stages of film casting. This collapse would assist diffusion of the relatively more flexible CAP chains out of the EC-rich phases. This is in agreement with the TBA data showing the presence of relatively purer EC-rich phases in the solid state. The same conclusion can be drawn from an equivalent argument based on changes in system viscosity. The concentration at which [deviation from equilibrium binodal decomposition commences is expected to be different for the two sides of the ternary phase diagram. Phase rearrangement in the EC-rich phase will deviate from equilibrium conditions at higher concentration than that of the CAP-rich phase. This assymetry will be expected to produce purer EC-rich phases when compared with the CAP-rich ones.

The asymmetric changes in the viscosity of the two phases will also lead to reduced viscosity of the matrix in EC-rich systems during film casting. This could potentially enhance coalescence of the CAP-rich dispersion during film casting. The micrographs do not show evidence of this process occurring to any significant extent. We believe this to be a result of the presence of CAP chains in the matrix (25–28% w/w) raising the overall matrix viscosity.

## CONCLUSIONS

EC and CAP have been shown to be incompatible at room temperature. Optical/electron microscopy and dynamic mechanical spectroscopy of films cast from 50/50 v/v methylene chloride/methanol have revealed the presence of two phases. The system remained heterogeneous even after annealing at temperatures above the $T_g$ of both homopolymers, confirming that the incompatibility is not associated solely with the solvent system used for film casting.

The solvent system is a cosolvent for one of the polymers (CAP) and a solvent/nonsolvent mixture for the other (EC). This is demonstrated by the

different adsorption characteristics of methanol and methylene chloride on the two polymers. Methanol interacts preferentially with CAP, possibly via the hydroxyls of the $\sigma$ carboxybenzoyl group, to form energetically, relatively more favorable 1-2-3 contacts at compositions 50/50 v/v of methylene chloride/methanol. On the other hand, methylene chloride interacts with EC solvating the chains. Changes in the solvent system composition during film casting are expected to influence the final film morphology through changes in the polymer conformation in solution, the viscosity, and consequently the diffusion of the two chains during phase rearrangement.

## REFERENCES

1. O. Wichterle and D. Lim, *Nature*, **185**, 117 (1960).
2. K. Petrak, *Br. Polym. J.*, **22**, 213 (1990).
3. N. B. Shah and B. B. Sheth, *J. Pharm. Sci.*, **61**, 412 (1972).
4. M. Donbrow and Y. Samuelov, *J. Pharm. Pharmacol.*, **32**, 463 (1980).
5. R. C. Rowe, *Pharm. Int.*, **6**, 14 (1985).
6. O. Olabisi, L. M. Robeson, and M. T. Shaw, in *Polymer-Polymer Miscibility*, Academic, New York, 1979.
7. P. Sakellariou, R. C. Rowe, and E. F. T. White, *Int. J. Pharm.*, **34**, 93 (1986).
8. P. Sakellariou, R. C. Rowe, and E. F. T. White, *J. Controlled Release*, **7**, 147 (1988).
9. P. Sakellariou, E. F. T. White, and R. C. Rowe, *Brit. Polym. J.*, **19**, 73 (1987).
10. T. G. Fox, *Bull. Amer. Phys. Cos.*, **1**, 123 (1956). (Also in the review of Equations for $T_g$-Composition Correlation, published by McKnight et al., in *Polymer Blends*, **1**, 188, AP, (1978).
11. P. Sakellariou, R. C. Rowe, and E. F. T. White, *J. Appl. Polym. Sci.*, **34**, 2508 (1987).
12. J. Prausnitz, R. N. Lichtenthaler, and E. G. Azevedo, in *Molecular Thermodynamics of Fluid-Phase Equilibria*, 1986, 2nd ed., Prentice-Hall, Englewood Cliffs, NJ 07632.
13. S. Krause, in *Polymer Blends*, Academic, New York, 1978, Vol. 1, p. 15.
14. P. Sakellariou, R. C. Rowe, and E. F. T. White, *Int. J. Pharm.*, **31**, 175 (1986).
15. H. Tompa, in "Polymer Solutions," Chap. 7, Butterworths, London, (1956).
16. V. Narashimhan, R. Y. M. Huang, and C. M. Burns, *J. Polym. Sci.*, **21**, 1993 (1983).
17. G. Allen, G. Gee, and J. P. Nicholson, *Polymer*, **1**, 56 (1960).
18. R. L. Scott, *J. Chem. Phys.*, **17**, 279 (1949).
19. D. Berek, D. Lath, and H. Aoki, *J. Polym. Sci.*, **C6**, 659 (1967).

20. V. Narashimhan, R. Y. M. Huang, and C. M. Burns, *J. Polym. Sci. Polym. Symp.,* **74,** 265 (1986).

21. V. Narashimhan, R. M. Huang, and C. M. Burns, *J. Appl. Polym. Sci.,* **37,** 1909 (1989).

22. C. Gonzalez, F. Zamore, E. Guterrez, J. R. Ramirez, and L. M. Leon, *Br. Polym. J.,* **22**(3), 155 (1990).

23. J. H. Hildebrand, J. M. Prausnitz, and R. L. Scott, in *Regular and Related Solutions,* Van Nostrand Reinhold, New York, 1970.

24. J. M. G. Cowie and I. McEwen, *Polymer,* **24,** 1449 (1983).

25. J. M. G. Cowie and J. M. McGrindle, *Eur. Polym. J.,* **8,** 1235 (1972).

26. J. M. G. Cowie and I. McEwen, *Macromolecules,* **7,** 291 (1974).

27. J. M. G. Cowie and I. McEwen, *J. Chem. Soc. Faraday Trans.,* **1,** 80, 905 (1987).

28. J. M. G. Cowie and I. McEwen, *J. Polym. Sci. Polym. Phys. Ed.,* **25,** 1501 (1987).

29. H. C. Van Ness and B. D. Smith, *Int. Data Ser. Sel. Data Mixtures Ser. A,* **1,** 24 (1984).

30. S. Murthy, R. P. Singh, and A. P. Kudghadker, *Indian Chem. Eng.,* **20,** 37 (1978).

31. G. C. Eastmond, C. Ming, and M. Malinconico, *Br. Polym. J.,* **19,** 275 (1987).

32. P. Sakellariou, G. C. Eastmond, and I. S. Miles, *Polymer,* to appear.